J. Physiol. (1987), **388**, *pp.* 323–347
With 14 *text-figures*
Printed in Great Britain

A FAST MOTILE RESPONSE IN GUINEA-PIG OUTER HAIR CELLS: THE CELLULAR BASIS OF THE COCHLEAR AMPLIFIER

BY J. F. ASHMORE

From the Department of Physiology, Medical School, University Walk, Bristol BS8 1TD

(*Received 2 July 1986*)

SUMMARY

1. Outer hair cells from the cochlea of the guinea-pig were isolated and their motile properties studied in short-term culture by the whole-cell variant of the patch recording technique.

2. Cells elongated and shortened when subjected to voltage steps. Cells from both high- and low-frequency regions of the cochlea responded with an elongation when hyperpolarized and a shortening when depolarized. The longitudinal motion of the cell was measured by a differential photosensor capable of responding to motion frequencies 0–40 kHz.

3. Under voltage clamp the length change of the cell was graded with command voltage over a range ± 2 μm (approximately 4 % of the length) for cells from the apical turns of the cochlea. The mean sensitivity of the movement was 2·11 nm/pA injected current, or 19·8 nm/mV membrane polarization.

4. The kinetics of the cell length change during a voltage step were measured. Stimulated at their basal end, cells from the apical (low-frequency) cochlear turns responded with a latency of between 120 and 255 μs. The cells thereafter elongated exponentially by a process which could be characterized by three time constants, one with value 240 μs, and a second in the range 1·3–2·8 ms. A third time constant with a value 20–40 ms characterized a slower component which may represent osmotic changes.

5. Consistent with the linearity shown to voltage steps, sinusoidal stimulation of the cell generated movements which could be measured at frequencies above 1 kHz. The phase of the movement relative to the stimulus continued to grow with frequency, suggesting the presence of an absolute delay in the response of about 200 μs.

6. The electrically stimulated movements were insensitive to the ionic composition of the cell, manipulated by dialysis from the patch pipette. The responses occurred when the major cation was K^+ or Na^+ in the pipette. Loading the cell with ATP-free solutions or calcium buffers did not inhibit the response.

7. It is concluded that interaction between actin and myosin, although present in the cell, is unlikely to account for the cell motility. Instead, it is proposed that outer hair cell motility is associated with structures in the cell cortex. The implications for cochlear mechanics of such force generation in outer hair cells are discussed.

INTRODUCTION

The mammalian cochlea separates different sound frequencies by an active and physiologically labile control of the basilar membrane motion (Sellick, Patuzzi & Johnstone, 1982; Khanna & Leonard, 1982; Davis, 1983). Experimental evidence from activation of the cochlear efferent system (Brown & Nuttall, 1984), the specific lesions produced by ototoxic drug and noise damage (Evans & Harrison, 1976; Liberman & Dodds, 1984) and theoretical models of cochlear mechanics (de Boer, 1983; Neely & Kim, 1986) all suggest that the outer hair cells of the cochlear partition are likely to be the force generators within the cochlea. In support of the idea of an active role for outer hair cells, it is known that hair cells are immunoreactive for a variety of contractile proteins (Flock, 1983) and manipulating the surrounding medium of hair cells produces relatively slow (time scale 10–100 s) alterations in the outer hair cell length. Such responses may be due to interactions of contractile protein systems or active rearrangement of the cell cytoskeleton (Zenner, Zimmerman & Schmidt, 1985; Flock, Flock & Ulfendahl, 1986). Nevertheless the difficulty with schemes which invoke such active movements to explain cycle-by-cycle force generation in the cochlea is that they may not operate fast enough: in some mammals such mechanisms may operate at rates exceeding 100 kHz.

Although study of outer hair cells has proved difficult *in vivo* (Dallos, Santos-Sacchi & Flock, 1982; Russell & Sellick, 1983; Dallos 1985), outer hair cells isolated *in vitro* from the cochlea show a remarkable motile response (Brownell, Bader, Bertrand & de Ribaupierre, 1985). Intracellular current injection by recording micro-electrode or stimulation with extracellular alternating current causes the cells to expand or contract, by amounts so large that the movement can be observed with a light microscope (Brownell *et al.* 1985; Ashmore, 1985). Nevertheless, such studies have been based on video recording techniques which limit the time resolution to below 30 Hz.

The present study uses patch recording techniques to study the properties of freshly dissociated hair cells from the adult guinea-pig cochlea. The dissociation procedure preserves the ultrastructural characteristics of the cells (Lim & Flock, 1985). The membrane properties of outer hair cells are now known to be dominated by a permeability to K^+ (Ashmore & Meech, 1986). It is shown here that isolated outer hair cells can change their length by up to about 4 % when current is injected into them. By using a photosensor system, it is found that the observed movement occurs at sufficiently high rates to be involved in acoustic tuning mechanisms. The results below confirm the findings of Brownell *et al.* (1985) but extend the time resolution to show that the first detectable movements in cells from the apical (low-frequency) cochlear turn can occur with an absolute delay of 120 μs. It is suggested that this high rate, and the insensitivity to internal Ca^{2+}, may rule out an an interaction between actin and myosin as the basis of motility.

The postulated role for an active element within the cochlear partition, at least in theoretical models of the cochlea, is to counteract the fluid damping of the cochlear partition (de Boer, 1983; Neely, 1983): simple passive motion of the basilar membrane cannot account for the degree of frequency selectivity possessed by the auditory periphery. Taken together with the organization of the organ of Corti, the

present quantitative measurements suggest that forces generated by outer hair cells may be sufficient to control the micromechanics of the cochlear partition and possibly to account for the active component required in theoretical models of the basilar membrane mechanics.

Preliminary reports on outer hair cell motility have previously been presented (Ashmore, 1985; Ashmore & Brownell, 1986).

METHODS

Cell preparation

Adult guinea-pigs (400–600 g) were killed by rapid cervical dislocation and both bullae removed. About 8–12 mm of the organ of Corti from the apical two turns were dissected using a fine needle into L-15 medium (lx, GIBCO; the major ions in the medium are (mM): Na^+, 135; K^+, 5; Ca^{2+}, 1·26; Mg^{2+}, 2; and amino acids, adjusted to pH 7·4). The tissue was transferred in a 70 μl aliquot to which was added 70 μl of L-15 with 1 mg trypsin/ml (Sigma type III). In some experiments, the basal cochlear turn was also used, but the yield of cells was lower. The dissection steps could be completed within 5 min. After 25 min, the droplet was gently triturated and diluted with a further 160 μl of L-15 in the experimental chamber. The chamber volume was maintained against evaporation by addition of distilled water (5 μl every 10 min). Cells could be used for up to 3–4 h after dissection. For this period they maintained their characteristic elongated shape, but subsequently deteriorated by rounding up and exhibiting a granular cytoplasmic appearance. Nevertheless, the second bulla could be kept, unopened, in moist tissue for subsequent use within about 6 h, with no apparent deterioration of cell properties. In this manner a total of up to about twenty cells could be studied from one animal. Some degree of enzyme pre-treatment was found helpful to obtain good patch seals. However, mechanical dissociation alone yielded cells which could be patched in the region immediately below the nucleus and responded to command steps indistinguishably from those enzymatically dissociated. Treatment with collagenase (Sigma type IV, 1 mg/ml for 10 min) was also used successfully to obtain cells from which patch recordings could be obtained. All experiments were carried out at room temperature (20–23 °C).

Recording methods

In these experiments conventional patch-clamp recording methods were used (Hamill, Marty, Neher, Sakmann & Sigworth, 1981). These extend micro-electrode studies (Brownell *et al.* 1985; Ashmore, 1985; J. F. Ashmore, unpublished) by allowing a much wider band width for the stimulus, and more precise control of the membrane potential.

Patch pipettes were pulled on a microprocessor-controlled two-stage puller (BB-CH, Mecanex), using 1·2 mm o.d. Pyrex glass, containing a filament (GC120F, Clarke Electromedical). They were back-filled and used immediately without further treatment. Such pipettes had access resistances between 15 and 40 MΩ because of the narrow taper. The pipettes used corresponded to 'bubble mark 4–6' with a typical internal tip diameter of 0·8–1·5 μm. Pipettes were positioned using a Huxley micromanipulator (Huxley–Bertram, Cambridge) possessing negligible drift. In early experiments a patch amplifier type EPC/5 (List Electronic, Darmstadt) was used but in later experiments an amplifier type EPC/7 was used allowing series resistance compensation of the pipette. Using a model of the cell and pipette, the amplitude and phase characteristics of command circuitry were estimated to be flat from 0 to 10 kHz to within 5 % and 18 deg respectively. Giga-seals could be readily obtained on the basal surface of the cell, where synaptic endings are made, and which enzyme treatment apparently clears. Seals could also be made, but with greater difficulty, on the lateral surface of the cell. The lateral surface of outer hair cells normally faces extracellular fluid in the spaces of Nuel and shows ultrastructural specializations, possibly anchoring the plasma membrane to the subsurface lamellae (Saito, 1983). This may produce differences in sub-membranous structures affecting the fluidity of the membrane and in turn the electrical pipette seal. Positive and negative pressure applied to the pipette was monitored using a small piezo-resistive pressure sensor (Lamb, Matthews & Torre, 1986).

The results reported here are based on the whole-cell variant of the patch recording technique

(Hamill *et al.* 1981). In this preparation, cell-attached recording conditions were established before creating whole-cell recording conditions. The membrane properties of the cells have been reported elsewhere (Ashmore & Meech, 1986; and in preparation). Outer hair cell membrane potentials are determined by predominantly a Ca^{2+}-gated K^+ permeability. With K^+, and Ca^{2+}–EGTA buffered to below 0·1 μM, in the pipette, the resting potential of the cells reported below was in the range -24 to -45 mV. When Na^+ replaced K^+, the resting potentials were in the range -3 to $+10$ mV. Most of the data described were obtained within 2–3 h after removal of the cochlea. Cells maintained in the chamber beyond 3 h tended to have lower resting potentials under the same recording conditions suggesting a developing leak conductance. The origin of this leak has not been explored. Movements could still be elicited in such cells, although with reduced amplitude. One explanation is that the potential drop across the pipette then became significant, and the membrane potential was poorly controlled. Data were not collected from cells with resting potentials more positive than -20 mV (pipette containing K^+).

Solutions

The pipettes were filled with a quasi-intracellular solution based on that used to study cultured rat myoball membrane (Magleby & Palotta, 1983). The solution contained: K^+, 140 mM; Mg^{2+}, 2 mM; Ca^{2+}, 0·1 μM (EGTA, 0·5 mM; Ca^{2+}, 0·279 mM); HEPES, 5 mM; titrated to pH 7·3 using KOH. In some experiments Na^+ replaced K^+, Ca^{2+} was buffered to levels below 10 nM using the calcium buffer bis(*O*-aminophenoxyl)ethane-*N*,*N*,*N*′,*N*′-tetraacetic acid (BAPTA; BDH) at 10 or 50 mM. Because the apical cells are large, some degree of internal Ca^{2+} buffering was used in the experiments to ensure that the current required to voltage clamp the membrane did not exceed the capabilities of the amplifier.

Determination of cell movements

Movement of the cuticular plate was determined by a photodiode pair sensing motion of a high-contrast boundary in the microscope image plane. The microscope was equipped with Nomarski optics, with illumination operated from a stabilized d.c. source. The beam was heat filtered (KG3 filter, Schott). The cells were observed at 640× magnification using a 40× water immersion objective (Zeiss, Oberkochen). A trinocular head (Leitz MPV system head) was used to align a photosensor on the cuticular plate of the cell by back-projection onto the viewed image plane. This photosensor consisted of a photodiode pair (LD-1-0, Centronics) with two parallel plates separated by 50 μm and arranged to detect differential illumination (Fig. 1).

The differential signal was amplified and frequency compensated to improve the band width. The effective photosensor band width was d.c. to 50 kHz (Ashmore, 1985; Howard & Ashmore, 1986). The response to a light step is shown in Fig. 1*B* and shows that the photodiode frequency response was flat in amplitude and phase from 0–20 kHz. The phase lag of the photodiode was 26 deg at 10 kHz. With full band width, the r.m.s. noise of the system alone corresponded to a movement of a high-contrast edge of 40 nm. A similar system, but with additional optical magnification, has been described in studies of turtle hair cells (Crawford & Fettiplace, 1985). In the present experiments, the quality of the optical image was quite variable, so that considerable variation in the signal-to-noise ratio was obtained. Signal averaging was employed to improve the signal. The photodiode output was recorded on FM tape (Racal Store 4) and then analysed off-line by computer.

The photosensor signal was operated to detect axial length changes of the cells. No signal could be obtained when the cells were imaged through crossed polarizers, indicating that the photosensor was not detecting a change in the birefringence of the cell. In addition, no signal could be obtained when the photosensor was positioned beyond the cuticular plate, indicating that fluid disturbance around the cell was not the main source of the photosensor signal. Because of the construction of the sensor, the output signal varied linearly with image movement, over a range of 4 μm, the largest movements encountered here. This was checked using a boundary edge moved in the beam by a piezoelectric bimorph (Fig. 1*C*). With an irregular edge, such as that of the cell, linearity over this range was also confirmed by moving the cell across the sensor using the manipulator. The absolute movement of the cell was calibrated visually by using an eyepiece graticule to measure the largest changes in cell length. In this case the accuracy is estimated to be about 20% ($\pm$ 0·3 μm).

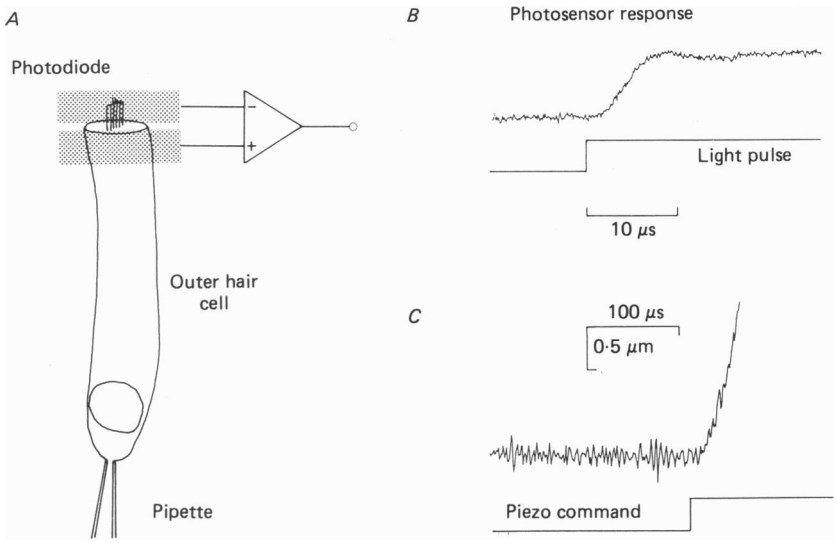

Fig. 1. Photosensor system for measuring rapid cell movements. *A*, Nomarski image of the cuticular plate was imaged onto a photodiode pair. The output was differentially amplified in photoconductive mode (feed-back resistor, 100 MΩ) and frequency compensated. *B*, step response of the photodiode to a light pulse generated by a 600 ns rise-time l.e.d. (light-emitting diode, RS part 306–077). The response settles in 12 μs. *C*, response of system to movement of a high-contrast edge in the image plane driven by a piezoelectric bimorph element. Command timing to element shown. The 13 μs lag is likely to have arisen from mechanical inertia of the bimorph.

Micrographic recording of cell movements

Video recordings of the cell were made (as in Fig. 2) with a camera (Sony AVC 3250CE, 550 lines horizontal resolution). A simple contrast-enhancement device was employed to stretch the video grey scale and to improve the resolution to the theoretical limit of about 0·2 μm. Since cell length changes were maintained during long (5–10 s) command steps, as described below, photographic exposures of the cells were also made. Although such methods were generally less successful in recording changes due to the vibration disturbance of the camera shutter, measurements from such photographs also confirmed the cell movements, and produced consistent estimates of the length changes. Measurement of the image density was made from high-quality video recordings (JVC U-matic Model CR6600E) by triggering a fast digital storage oscilloscope at the start of a selected single raster line.

RESULTS

When hyperpolarizing, or depolarizing, current was injected into the cell through the patch pipette, the cell elongated or shortened, respectively (see Fig. 2). For command voltage steps of 100 mV, of either polarity, these movements were typically of about 1–2 μm in amplitude.

Shape changes elicited in the cell

The simplest observations suggested that movements occurred at constant volume (a further quantitative argument is presented in the Discussion). Although the length change was most prominent (Fig. 2) the elongation in some cells was associated with

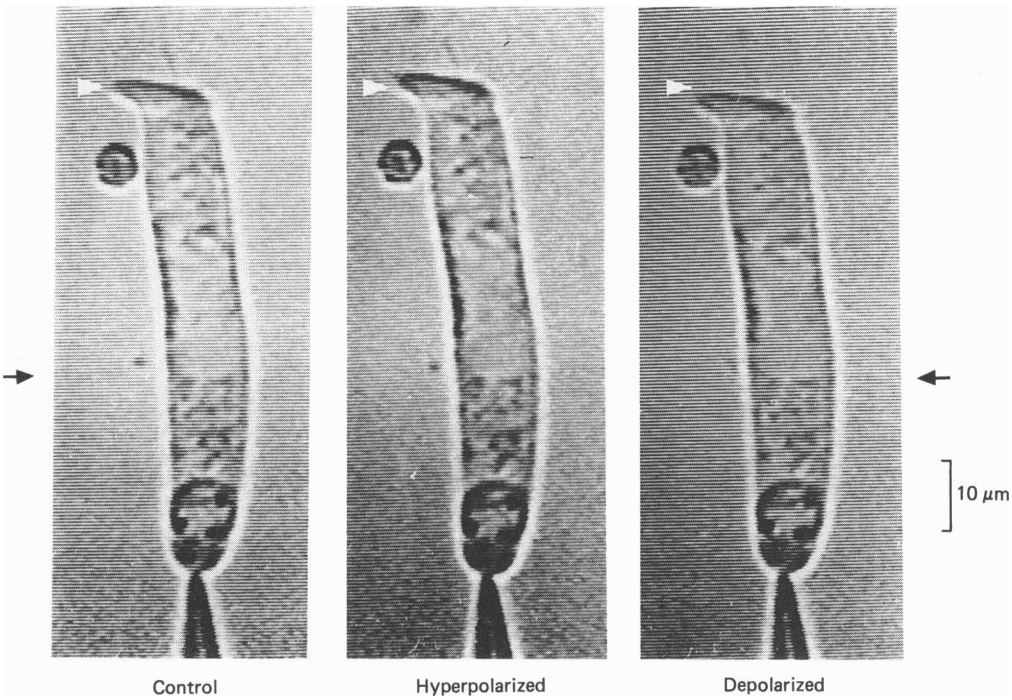

Fig. 2. Alteration in shape of an isolated outer hair cell at rest (left), during hyperpolarizing (middle) and during depolarizing (right) command steps. Single frames taken at 2 s intervals from a video-enhanced contrast image. The open arrow mark is at the same distance from the pipette at the base in each frame. Command (±90 mV) applied via the patch pipette recording in whole-cell mode at the cell base. Cell diameter changes (Fig. 3) measured between closed arrows.

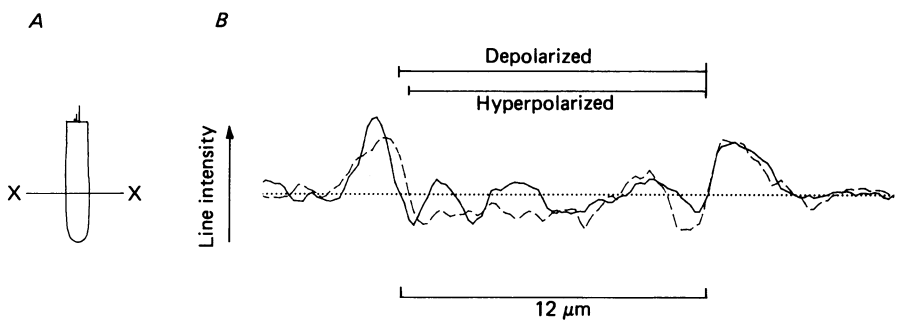

Fig. 3. Diameter change in outer hair cells with stimulation. Scan of video intensity across cell shown in Fig. 2 during −90 mV (continuous line) or +90 mV (dashed line) command pulse. *A*, video raster line position, 40% from base along cell, marked X–X. Position arrowed on Fig. 2. Cell diameter at this position, 12 μm. *B*, line intensity (arbitrary units, white upwards) *vs.* position. The cell boundaries appear as a white–black band arising from the diffraction pattern on the (video contrast-enhanced) Nomarski image. The dotted line corresponds to the background grey level of the picture. The cell diameter was 0·2 μm less when the cell was hyperpolarized. Video raster line digitized at 50 ns per point (equivalent to 0·5 pixel per sample).

a narrowing of the cell around its mid region between the nucleus and the cuticular plate and conversely, when the cell shortened, this same region often bulged slightly.

Fig. 3 shows the changes of diameter of the central portion of the cell that were measured using video densitometry on the cell shown in Fig. 2. The cell diameter was approximately 0·2 μm less when the cell was hyperpolarized than when it was depolarized. This corresponds to a diameter change of approximately 1·7 %. Although close to the resolving power of the microscope, changes of this magnitude were seen consistently in video records. It is the change expected if the cell maintained volume: in that case, the fractional diameter change would be 0·5 times the fractional length change. From the length changes of 4 % described below, the diameter change would thus be about 2 %. In the quantitative measurements described below, only the vectorial component perpendicular to the apical surface will be described. This is estimated to be over 80 % of the resultant motion in all cells studied even though in some cells which exhibited a noticeable curvature, a bending motion of the cell could also be seen.

Recording from the cell came to an abrupt end when the nucleus was ejected (Brownell *et al.* 1985) either from the basal or from the lateral region of the cell. This often occurred after large depolarizing steps. There was then a sudden rise in cell input conductance, indicating rupture of the cell membrane, and usually the nucleus appeared to be 'squeezed out' while the cell elongated over a period of 5–10 s. One possible explanation for the elongated cell shape is that internal pressure maintains the cell's shape and length. Had the nucleus been ejected by a large intracellular pressure, it might be expected that the cell would then have shortened or collapsed as the internal pressure was relieved. Instead the cell invariably lengthened.

The simplest explanation is that the mechanical responses involve a circumferential tension which maintains the cell in a cylindrical form. In addition, there must also be an opposing longitudinal force so that both reversible elongation and shortening occur. In support of this hypothesis, small positive pressures (2–5 Pa) applied to the pipette produced a 10–20 % shortening of the cell even though movement could still be elicited. However, although apical cells possess a pronounced cytoskeletal web which extends down from the cuticular plate to near the nucleus (Lim & Flock, 1985) this observation suggests that such structures are not directly involved in the movement. There was no pronounced alteration in the angle of the cuticular plate. It is more likely that the movement is associated with the cell cortex, possibly the characteristic subsurface cisternae of outer hair cells or the associated membrane. It should be noted that alteration of the tension in the cell cortex would lead to a change in the length of the cell since the forces generated would be coupled through the incompressible fluid cell contents. This model, consisting of two coupled spring systems, will be further examined in the Discussion section.

The above observations thus suggest that the shape change in outer hair cells may be similar to that of an elastic cylinder, lengthening as its diameter is reduced.

The effect of stimulation at other sites on the cell

Cells were usually recorded with a patch pipette on the basal end of the cell. However, it was found possible to patch the lateral surface of the cell near the cuticular plate or in the middle of the cell itself. Movements were also generated under

these conditions with the same stimulus polarity. When stimulated in the middle, both ends of the cell would move in antiphase. The magnitude and sensitivity of the movement was indistinguishable from that found with stimulation at the base. It must therefore be concluded that the movement does not depend on the polarity of the current flowing longitudinally along the cell, but is likely to depend either on the transmembrane current or potential. Current is injected *in vivo* into the cell through the mechano-electric transduction channels at the apical end. In these experiments, where current is injected at the basal end of the cell, it will be assumed that the movements are kinetically independent of the stimulation site.

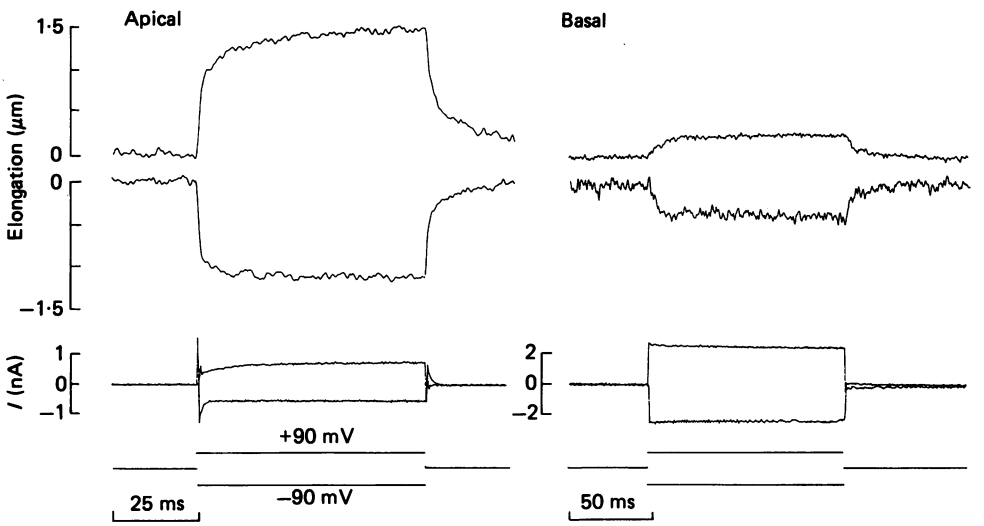

Fig. 4. Movement signals from apical and basal outer hair cells. Whole-cell recording, voltage clamp. Cells were isolated in two separate droplets from respectively, the apical two turns and the basal turn, from the same animal. Pipette contained: K^+, 140 mM; Ca^{2+}–EGTA, 0·01 μM. Cell resting potentials: apical cell, −44 mV; basal cell, −38 mV. Command steps 90 mV from rest. Photosensor responses (upper traces) were signal averaged: apical cell, 64×; basal cell, 128× (hyperpolarizing), 40× (depolarizing). Photosensor output low-pass filtered at 880 Hz.

Responses of apical vs. basal cells

The site of origin of isolated guinea-pig hair cells can be determined by the length of the cell body and stereocilia. Cells from the apical cochlea (low-frequency end) are longer (60–80 μm) than from the basal cochlea (cell length 15–30 μm). Fig. 4 shows that outer hair cells from both apical and basal cochlear turns responded to a command voltage step. While the cell from the apical cell changed length by ±2 μm, the maximum change in length obtained from basal cells was usually much less, typically ±0·5 μm. The basal cell, 27 μm long, was 35 % of the length of the apical cell (76 μm) indicating that the length change is graded with length of the cell. The maximum excursion was 3·8 and 4·0 % of the total length for the basal and apical outer hair cells, respectively. A maximum length change of about 4–5 % of the length was found in the majority of the cells studied.

Because the cells from the apical two turns isolate most readily, and the observable movement is largest there, this population of cells will be studied below.

The movement is graded with stimulus

By placing the photosensor over the cuticular plate, the movement of the apex relative to the (fixed) base was measured during changes in the voltage command.

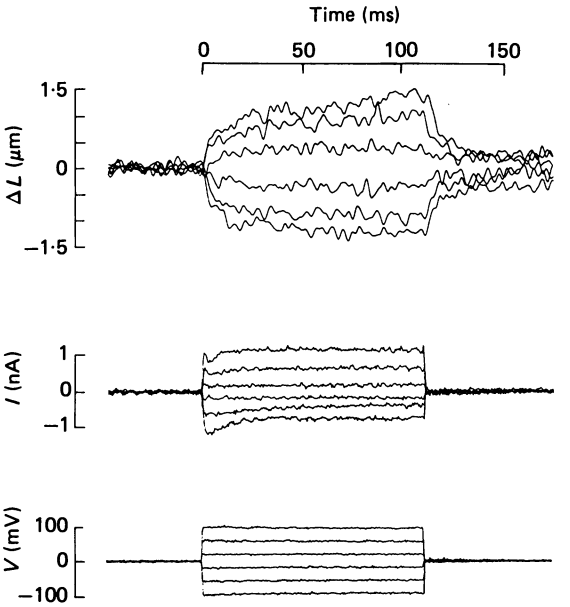

Fig. 5. Graded nature of length changes. Cell voltage clamped, whole-cell recording. Top, photosensor output, ten sweeps averaged for each trace. Data low-pass filtered 880 Hz. Middle, clamp current. Bottom, voltage command. Pulses in increments of 36 mV from −90 to +90 mV, delivered at 1·2 Hz. Holding potential, −50 mV. Cell resting potential, −42 mV. Recording pipette series-resistance compensated (60%).

Fig. 5 shows the length change, ΔL, of a cell held under voltage clamp near its resting potential (−42 mV). Command voltage steps around the resting potential were applied and the cell elongated when hyperpolarized and shortened when depolarized. The movement appeared to be a low-pass filtered version of the command pulse and will be further analysed below.

Fig. 6*A* shows that the response was graded linearly with the magnitude of the injected current for movements less than about ±1 μm. There was no detectable threshold stimulus below which no movement occurred. Beyond this range it was noted that the movement saturated (Fig. 7). The sensitivity of the motion was 2·2 nm/pA injected current in the cell shown. In a sample of seven cells the mean sensitivity to current was 2·11 ± 1·19 nm/pA (mean ± S.D). The equivalent sensitivity to voltage was also determined. For the cell shown in Fig. 6*B*, it was 25·6 nm/mV applied polarization around rest. The sample mean was 19·8 ± 8·3 nm/mV. As seen in

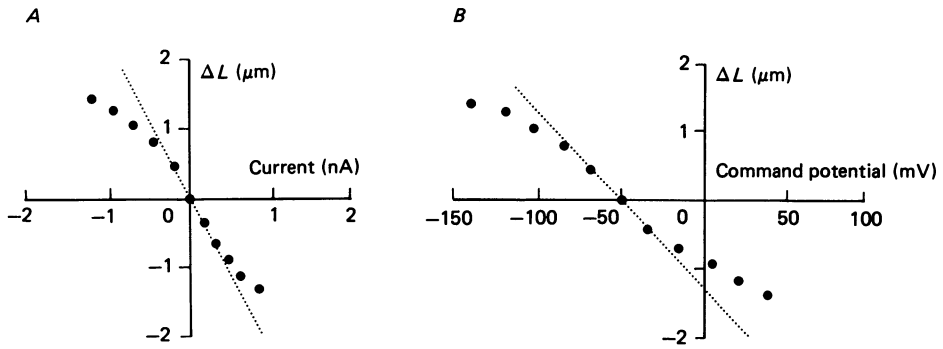

Fig. 6. Graded nature of length change from rest. *A*, length change *vs.* clamp current. Cell shown in Fig. 5. Maximum elongation, 1·6 μm. Slope, 2·2 nm/pA. *B*, length change *vs.* command potential. Slope, 26 nm/mV. Resting cell length, 63 μm. Pipette contained 140 mM-K^+, 0·1 μM-Ca^{2+} (EGTA buffered).

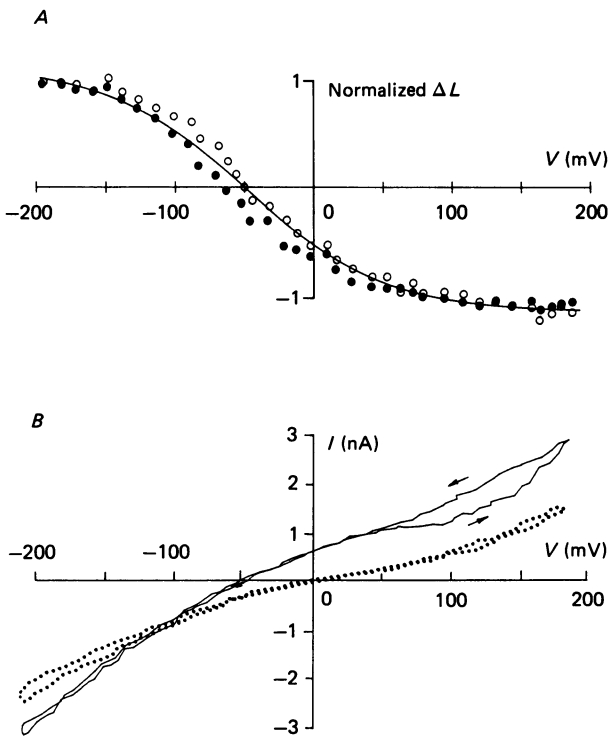

Fig. 7. Independence of length change to dialysing medium. Whole-cell recording, voltage clamp. Command potential was ramped at 0·4 mV/ms from −200 to 150 mV; holding potential, −50 mV. Two cells shown, from same cochlea. ●, pipette contained 140 mM-K^+ and 1 mM-EGTA; cell resting potential, −39 mV; input conductance, 13 nS; ○, pipette contained 140 mM-Na^+ and 0·25 μM-Ca^{2+}–EGTA; cell resting potential, +2 mV; input conductance 9 nS. *A*, single sweeps of photosensor output, filtered at 220 Hz. *B*, simultaneous *I–V* curves of cells (continuous lines, K^+ pipette (140 mM-K^+); dotted lines, Na^+ pipette (140 mM-Na^+)). Arrows show the direction of the current ramp (one cycle). The continuous line in *A* is drawn according to eqn. (3) of Discussion section, with $a = 1/51$ mV, $V_0 = -50$ mV.

Fig. 7, the membrane is approximately ohmic around the resting potential (Ashmore & Meech, 1986) and thus this type of experiment cannot determine whether it is voltage or current which controls the movement.

Dependence of the movement on cell contents

When cells were held at holding potentials outside the range −100 to +20 mV the amplitude of the movement was substantially reduced.

Fig. 7 shows the result of an experiment in which a cell was held at −50 mV using a pipette filled with 140 mM-K^+, and the potential ramped at 0·4 mV/ms around those points. Under these conditions (Fig. 5*B*) the current–voltage curve is non-linear, showing outward rectification maximal between +50 and +100 mV characteristic of the presence of a Ca^{2+}-gated K^+ current (Ashmore & Meech, 1986). The photosensor signal from the cell showed saturation when the potential was increased by more than about 70 mV in either direction from the holding level. Fig. 5*A* shows that the movements could also be elicited in the physiological membrane potential range between −90 and −70 mV, close to the resting potential of hair cells *in vivo* (Dallos *et al.* 1982; Cody & Russell, 1985).

Fig. 7 also shows that responses of the cells could be obtained when the cell was internally dialysed with Na^+ via the pipette. The movement was observed when the recording pipettes contained standard solution containing 140 mM-K^+ or when the Na^+ replaced K^+ in the pipette. Under these conditions, the cell resting potential typically reached a steady state of either −25 to −45 mV (K^+ pipette) or −3 to 10 mV (Na^+ pipette) indicating that equilibration between the cell and pipette contents had occurred. (Separate experiments using dye filling also indicated that the contents of the pipette and the cell equilibrated over about 2–3 min.) Fig. 7*B* shows that the *I–V* curves of cells differed, with a shift in the resting potential and a reduction of the input conductance in Na^+-dialysed cells. However, no significant differences in the magnitude length change, ΔL, were observed in twelve cells studied. A small shift in the curve of ΔL *vs.* potential was observed in this case (the mid-point of the curve shifting by about 10 mV). This shift was not exhibited consistently in the twelve cells studied in this manner.

In addition to K^+–Na^+ replacement, the effects of differing Ca^{2+} levels in the pipette were investigated. Normal recording pipette solutions contained 0·1 μM-Ca^{2+} (EGTA buffered, see Methods). In later experiments, EGTA was replaced by BAPTA (Ashmore & Meech 1986). In some experiments, 10 mM-BAPTA was included in the pipette, which, assuming equilibration between pipette and cell, should have reduced the intracellular Ca^{2+} concentration to below 10 nM. Such manipulations failed to stop the movements. In addition, since no ATP was included in the pipette filling solution, it must be assumed that the motion occurred in the absence of normal substrates for the actomyosin cycle.

Kinetics of the length change

In Fig. 6 it was observed that the movement was graded and that the length changes appear to be characterized by several exponential time constants. Figs. 8 and 9 show in particular that both the elongation (and shortening from negative holding levels) during pulse hyperpolarizations of 90 mV are characterized by at least

two time constants of 2·8 and 22 ms (Fig. 8*B*). The smaller of the two time constants was also determined by a peeling procedure, and found to differ by less than 10% from the estimate above. The similarity of the relaxation at both command onset and offset, also suggests that the mechanism rates do not depend on the absolute membrane potential.

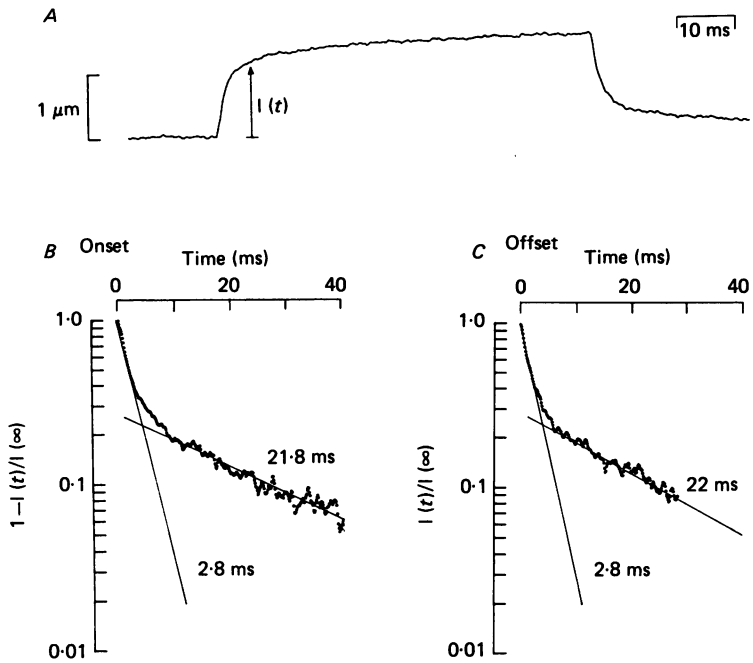

Fig. 8. Time course of the movement following a command pulse. Whole-cell recording, voltage command −90 mV, from rest −32 mV. Same cell as in Fig. 4 (apical). *A*, photosensor output, 512 samples averaged, 40 ms pulse, 880 Hz filter. *B*, semilogarithmic plot of response rise. $l(t)$ is the magnitude of the photosensor output from the base line. Time constants indicated by each fit to data. *C*, as in *B*, semilogarithmic plot of $l(t)/l(\infty)$, at offset of the command. Resting cell length, 77 μm.

Although the relative contributions of the two exponential components varied from cell to cell, neither of them is likely to be due to the clamp time constant. Although the cell capacitance was charged through the patch pipette, amplifier series resistance compensation was employed to reduce this time constant to 0·7 ms in the cell shown. In other cells studied, the smallest of the time constants was consistently 2–3 times larger than that characterizing the charging of the cell membrane, typically 1·3 ms (Fig. 12).

Rate of the elongation

If outer hair cell movements are to be involved in cochlear processes, then the movement should occur at rates corresponding to acoustic frequencies. Fig. 9 shows, on a faster time scale, the response of a cell (the same cell as in Fig. 8) to a −90 mV

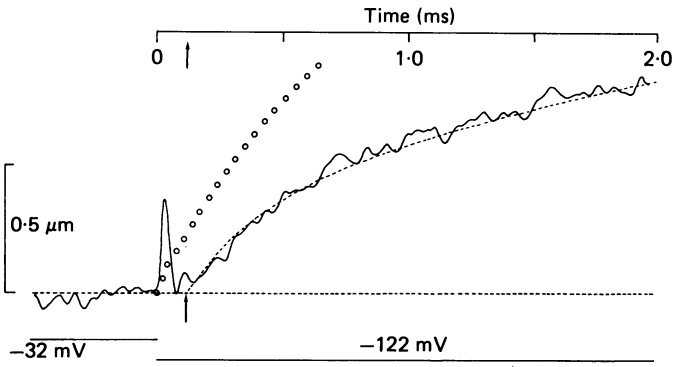

Fig. 9. Latency of the response. Cell as in Fig. 8, but on an expanded time scale. 512 samples signal averaged, sampled at 2·5 μs/point. Band width of photosensor signal, d.c.–20 kHz. At onset of the −90 mV command step, a 0·5 μs switching transient was generated in the recording system, and used to mark the command onset; the low-pass Bessel filter (3 dB point, 28 kHz) of the tape-recorder converts it to a pulse which lasted for the first 50 μs of the signal. The curved dashed line is the function $l(t-120\ \mu s)$ given in eqn. (1). The open circles plot movement which would follow intracellular potential. The time constant, 0·7 ms (measured from the current monitor) is that expected for an equivalent *R–C* cell circuit. The normalization is determined by the requirement that the voltage determines a final elongation of 1·4 μm. See text.

hyperpolarizing command step which caused an elongation of 2 μm. This result shows that a simple exponential analysis of the elongation rate requires modification at short times. The rise of the signal started from the base line at 120 μs (arrowed). It then increased at a rate which could be characterized by an exponential time constant of 150 μs. The data were fitted by a 'delayed' function $l = l\ (t-120\ \mu s)$ where (in μm):

$$l(t) = 2-0{\cdot}28\exp(-t/240\ \mu s)-1{\cdot}12\exp(-t/2{\cdot}8\ ms)-0{\cdot}6\exp(-t/22\ ms). \quad (1)$$

The last two exponential terms reflect time constants determined in Fig. 8. Their additivity suggests that two different processes may be occurring in parallel, the longer time-constant process possibly reflecting electro-osmotic processes (Terakawa, 1985). Fig. 9 shows that $l(t)$ is distinct from that predicted from the membrane potential rise. The first exponential term may arise solely from the exponential fitting procedure and a more likely explanation is that $l(t)$ describes a complex viscoelastic motion of the cell which bears formal similarities to electrotonic propagation along a cable. Nevertheless, the exponential fit provides a prediction for the response to sinusoidal commands (see below).

The response can thus be fitted to a curve $l(t)$ characterized by at least three time constants, differing from one another by an order of magnitude, as well as by an absolute delay. Fig. 1*B* shows that this delay was not due to a delay in the detection apparatus since at comparable band width (0–40 kHz) the delay in the photosensor was 13 μs, an order of magnitude faster. In ten cells from the apical turn (cell length 63–85 μm) the measured delay was 182 μs with a range of 120–255 μs. Measurements were made on cells which were attached to the chamber base; the time constants were much more variable, with rather longer associated delays (greater than 1 ms). For

comparison, the estimated potential rise in the cell is shown, based on the assumption that the charging rise curve monitored by the patch amplifier gives the correct circuit time constant (0·7 ms, 60 % series compensation).

Because of the lower signal-to-noise ratio in cells from the basal region the kinetic analysis was not extensively carried out. However, in three cells analysed, a delay preceding elongation was less than 100 μs, and possibly shorter than the temporal

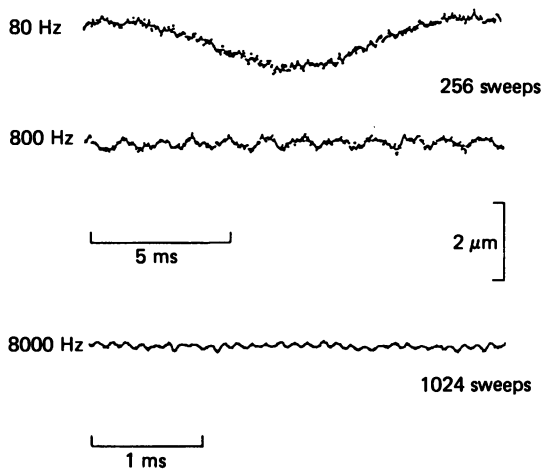

Fig. 10. Response of the cell to sinusoidal command stimuli. Whole-cell recording, voltage clamp. Sinusoidal voltage commands, 75 mV peak-to-peak amplitude, applied to the cell with 80 % pipette series-resistance compensation applied. Signal averages, number of sweeps indicated. Recording pipette contained 140 mM-K^+, 10 mM-BAPTA, pH 7·4. Holding potential, −40 mV.

resolution of the measuring system. It may thus be concluded that the motion of the cuticular plate is not instantaneous under these conditions but may involve an absolute delay, possibly arising from a propagation delay of a movement signal down the cell. Delays due to electrotonic voltage spread down the cell are estimated to account for only about 40 μs (J. F. Ashmore & R. W. Meech, in preparation). If it is assumed that motion originates in the middle of the cell, 35 μm from the cuticular plate, then a 180 μs delay could be produced by a propagation velocity of 1·9 m/s. Comparable velocities have been reported for the propagation of a pressure wave in the squid axon (Terakawa, 1985).

Since the motion depends linearly on the stimulus, an equivalent type of experiment was performed with the cells stimulated by a sinusoidal command.

Fig. 10 shows the result of an experiment using a sine-wave command potential with an amplitude of 75 mV. At low frequencies, the motion of the cell was sinusoidal. This behaviour is consistent with the linearity of the response mechanism apparent with step commands (Fig. 5). At frequencies above 800 Hz, signal averaging revealed a response but attenuated in amplitude.

Fig. 11 shows a quantitative analysis of these measurements. The amplitude of the photosensor output falls from 30 Hz to 1 kHz approximately as frequency$^{-1/2}$ (3 dB

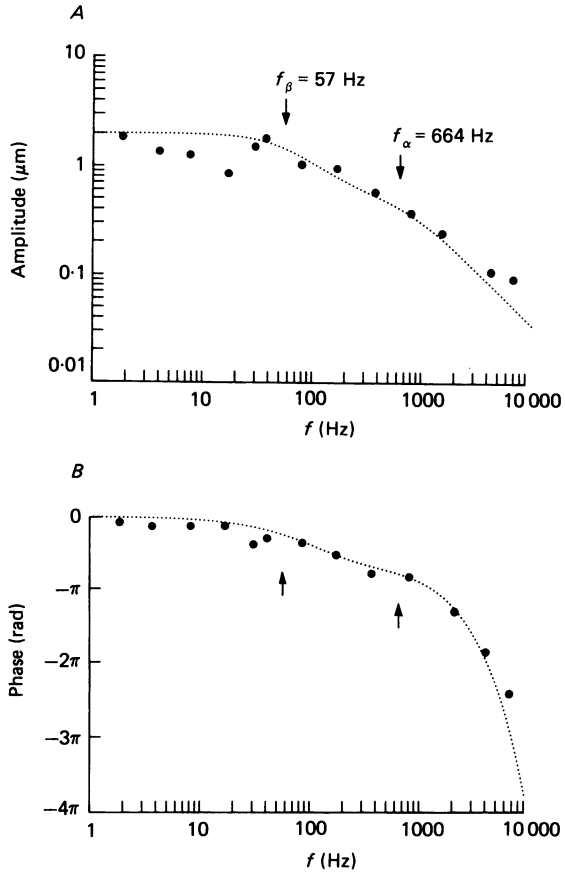

Fig. 11. Amplitude and phase of movement for cell of Fig. 10. *A*, peak-to-peak amplitude of photosensor signal obtained from signal-averaged records. The dotted line is the amplitude $\tilde{I}(\omega)$ computed from eqn (2) scaled for this cell. Frequencies f_α, f_β, corresponding to time constants τ_α, τ_β are arrowed. Because of the two components, the data points appear to fall on an approximately 3 dB per octave slope line up to 1 kHz. *B*, phase of signal relative to sinusoidal command voltage stimulus. The dotted line is the phase lag computed from Arg $(\tilde{I}(\omega))$ allowing for an absolute delay of 180 μs. The total contribution to the phase lag from the amplifier command and recording electronics was less than 20 deg at 10 kHz.

per octave). Thus at 1 kHz the amplitude of the movement in this cell was 0·2 μm. Nevertheless, this behaviour is predicted from the response to step pulses. The complex amplitude of the response to sinusoidal stimulation is obtained from Fourier transformation of $I(t)$, eqn (1), the response to a short pulse, and is given by

$$\tilde{I}(\omega) = \exp(-i\omega T)\left(\frac{0{\cdot}28}{1+i\omega\tau_\alpha} + \frac{1{\cdot}12}{1+i\omega\tau_\beta}\right), \tag{2}$$

where $i = \sqrt{-1}$, the angular frequency, $\omega = 2\pi f = 2\pi \times$ stimulus frequency, the absolute delay, $T = 120$ μs and $\tau_\alpha = 240$ μs and $\tau_\beta = 2{\cdot}8$ ms are exponential time constants of eqn. (1). The amplitude and phase of $\tilde{I}(\omega)$ are plotted in as dotted lines

in Fig. 11*A* and *B*, respectively. It should be noted that if the viscosity of the surrounding medium had been sufficiently high to damp the end motion of the cell, the frequency (f) dependence of the amplitude should have declined as f^{-1}. One interpretation is that forces generated within the cell to change its length are greater than the force generated externally by viscous fluid damping (see Discussion).

Fig. 11*B* shows that the phase of the photosensor output begins to exhibit a lag at around 60 Hz, but does not increase until the frequency exceeds 1 kHz. This behaviour is not that predicted by simple external viscous damping which would predict a phase asymptote at 90 deg phase lag. Instead the phase lag beyond 60 Hz continued to grow. At 1 kHz the phase lag was 180 deg and at 4 kHz was greater than 360 deg. Such behaviour is characteristic, for example, of an absolute delay in the system although distributed filter, mechanical or electrical, can also produce such behaviour. The dotted line is the phase shift predicted from Arg ($\tilde{I}(\omega)$) with an absolute delay, T, of 180 μs. Such a delay produces a better fit than $T = 120$ μs required for the cell in Fig. 9, but is within the range of the delays found for the population of cells.

Capacitance of the cell membrane

An ultrastructural characteristic which distinguishes outer hair cells from inner hair cells, and other cells within the cochlear partition, is the presence of a system of prominent cisternae below the surface plasmalemma. It is of interest to know whether these cisternae are in electrical contact with the surface membrane. Using patch recording, the membrane capacitance of the cell can be readily determined. Fig. 12 shows the charging curve of an outer hair cell immediately before and following the establishment of whole-cell recording conditions. In this experiment the pipette was voltage clamped at 0 mV. A 20 mV test pulse was applied during cell-attached recording conditions and the transients compensated. Trace *b* shows the current flowing into the cell to charge the membrane capacitance. The initial current transient was characterized to within experimental accuracy by a single-exponential charging curve with a time constant of 1·3 ms (Fig. 12*B*).

Fig. 12 shows that an outward current was required to maintain the cell at 0 mV. From *b* the initial input conductance of the cell was 4·5 nS, and the initial cell resting potential, −18 mV, within the range reported by micro-electrode studies (Brownell *et al.* 1985; J. F. Ashmore, unpublished). The outward current steadily increased to 80 pA over 1–2 min after establishing whole-cell recording. The most likely explanation is that K^+ diffused into the cell from the pipette, to establish a resting potential of −33 mV (Ashmore & Meech, 1986). From the area under the exponential charging curve and correcting for the cell input resistance, the cell input capacitance is computed to be 29·0 pF.

In six other cells of comparable dimension (i.e. 60–75 μm long) the cell input capacitance was estimated to be 27·3 ± 6·0 pF (± S.D.). The exponential charging curve time constant was 1·29 ± 0·48 ms (± S.D.). If the cells are modelled as a cylinder of diameter 10 μm and 70 μm long, with a specific membrane capacitance of 1 μF/cm^2, the input capacitance would have been 23·6 pF. Including the membrane of 100 stereocilia, 0·3 μm in diameter and 6 μm long, increases the input capacitance to 29·2 pF. This is sufficiently close to the experimental estimate to rule out

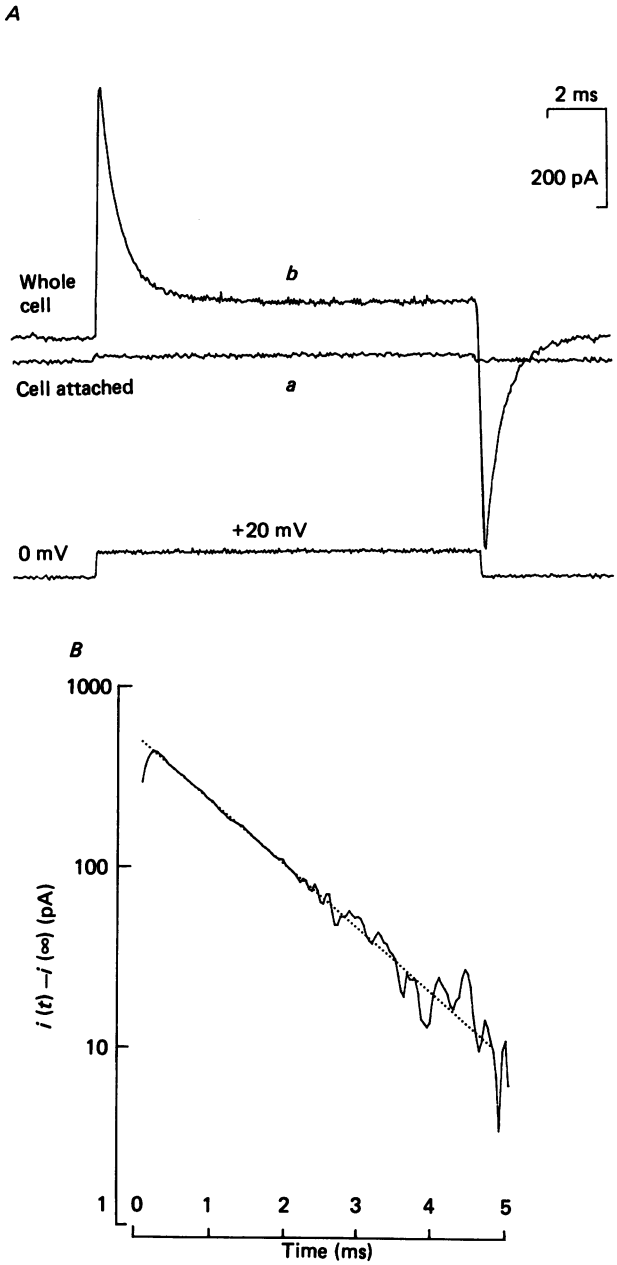

Fig. 12. Capacitance of the cell membrane. *A*, patch pipette current in the cell-attached mode (*a*) and immediately after establishing whole-cell recording (*b*). Holding potential 0 mV, test pulse 20 mV. In *a*, the pipette transients were fully compensated. Recording band width, 3 kHz. *B*, decline of pipette current. A single exponential fits the data, time constant 1·3 ms.

contributions to the input capacitance from additional membrane not included in the cell outline. Thus these measurements exclude a low-resistance pathway or membrane continuity between the plasma membrane and the subsurface cisternae.

DISCUSSION

The results show that outer hair cell motility, the ability of the cell to deform its shape at frequencies above 1 kHz, exhibits a number of properties that are required to explain the cellular basis of the 'cochlear amplifier' (Davis, 1983). It is now appreciated that a purely passive basilar membrane is incapable of reproducing the frequency-selective properties of the cochlea (de Boer, 1983). Most theoretical models for active basilar membrane mechanics require components within the cochlear partition which are capable of modifying the motion of the basilar membrane, possibly within one cycle.

Some of the properties possessed by outer hair cells relevant to this mechanism will now be considered. Although all experiments reported here were performed at room temperature, experiments were also performed at 37 °C (J. F. Ashmore, in preparation) which suggest that the underlying motility is relatively temperature insensitive (Q_{10} = 1·2–1·5). The report that temperatures below 30 °C severely affect the mammalian frequency tuning mechanisms (Brown, Smith & Nuttall, 1983) must therefore imply that the critical temperature-dependent site is located elsewhere within the cochlea, for example in the stria vascularis which maintains the endocochlear potential.

Outer hair cells and the geometry of the cochlear partition

Outer hair cells are organized in arcs centred on a point near the base of the inner hair cells and the basal foot of the inner pillar cell. This is where the modiolar edge of the basilar membrane may pivot (Davis, 1965; Zwislocki, 1980; Lim, 1980; Miller, 1985). Gently curved outer hair cells are prominently found amongst the cells isolated from the apical turn of the cochlea. Such organization suggests that outer hair cells generate forces which would act perpendicularly to the basilar membrane and thereby influence its motion. The arc-like configuration of outer hair cells would ensure that a constant couple would be exerted on the basilar membrane (relative to the foot of the inner pillar cell) while decoupling the shear displacement produced by motion and activating the mechano-electric transducer in the stereocilia. Such organization is less prominent in the basal turn, however, where the cells are shorter.

The movements described in the Results indicate that the cells are capable of generating forces over the same scales as would occur near auditory threshold (0·1–1 nm; Sellick *et al.* 1982). In addition, the polarity of the motile force is of the correct sign to increase the motion of the cochlear partition: movement of the basilar membrane towards scala media would open transducer channels, depolarize the cell and thus produce a force which would further pull the basilar membrane towards scala media. The opposite would happen when the basilar membrane moves towards scala tympani. In such cases hair cell force generation can be seen as augmenting the motion of the basilar membrane. Formally, in a model of the cochlear partition, this would be represented as a mechanical element represented as an impedance, Z_{ohc},

contributing a negative stiffness acting on the basilar membrane motion. The results suggest, however, that the stiffness is not instantaneous, and so the element would have a reactive component as well. Components of the force generated by an outer hair cell would thus be 90 deg out of phase with the basilar membrane displacement and would thus oppose the fluid damping on the membrane. Such requirements are the basis of 'negative damping' models of cochlear micromechanics (Neely & Kim, 1986) and calculations based on such types of model have been reported in outline (Neely, 1983; Geisler, 1986).

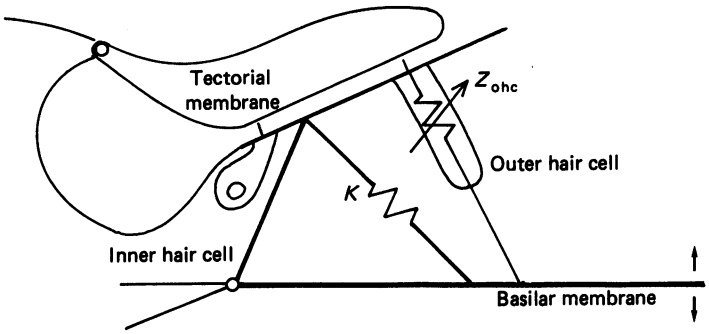

Fig. 13. Schematic model of the cochlear partition. K represents the stiffness of the partition. Z_{ohc} represents the mechanical impedance, which may include reactive elements, of the system of outer hair cells. See text.

Miller (1985) and Gummer & Johnstone (1981) have measured the static compliance of the basilar membrane, at the basal end of the cochlea. These studies have suggested that the organ of Corti may contribute to the static compliance of the basilar membrane. Such measurements may be summarized by placing a spring of stiffness $K = 2{\cdot}4\ \mu N/\mu m$ near the base of the outer pillar cell (Fig. 13). Thus any forces sufficient to influence the static basal basilar membrane mechanics should also be of this order, although dynamic behaviour may involve forces significantly smaller.

The compliance of the stereocilial bundle in a variety of hair cells has now been determined (Strelioff & Flock, 1984; Crawford & Fettiplace, 1985; Howard & Ashmore, 1986) with fairly good agreement for the strength of the pivotal spring. The sensory hair bundle in mammalian hair cells behaves like a sprung pivoted rod: in outer hair cells from the apical turn, the bundle will resist displacement with a force of about 1 nN per micrometre displacement of its tip. However, although there is a mechanical advantage when the stereocilia are driven by the basilar membrane, there is a lever disadvantage for a couple on the apex of the hair cells to influence the basilar membrane motion (typically a reduction of the couple by 6–10 times, Rhode & Geisler, 1967; Allen, 1980). The static couple which the stereocilia could exert on the basilar membrane would thus be too small by 2–3 orders of magnitude. This consideration also suggests that it is the forces generated along the outer hair cell axes which influence the basilar membrane micromechanics.

Forces generated by outer hair cells

Isolated outer hair cells change shape and length against viscous forces of the surrounding medium as well as against internally generated forces arising from surface tension, shear and bending stresses of the cell cortex and cytoplasm. Since *in vivo* outer hair cells are arranged with their apical surfaces joined into the plate of the reticular lamina and their basal ends inserted into the processes of Dieters' cells such motion is likely to be partially constrained, and the cells would be generating forces in near-isometric conditions. Since less work would then be done against internal viscous forces, the longitudinal forces generated by the cell would be larger than generated during unconstrained motion. Some of these forces can be estimated.

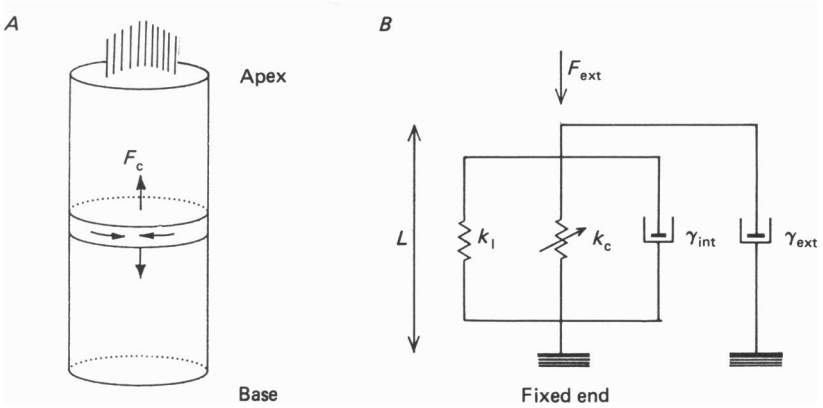

Fig. 14. Equivalent mechanical model of the outer hair cell. *A*, forces arising in cell. In a hydrostatically closed cell, a change in tension of each circumferential element gives rise to a longitudinal force component F_c. In addition, intrinsic longitudinally oriented forces are presumed to act within the cell cortex. *B*, equivalent model showing stiffness and viscous elements controlling cell length, *L*. See text.

The simplest model which summarizes the present findings is shown in Fig. 14. This model for the cell length L contains two springs. One spring, with stiffness k_l, represents the intrinsic longitudinal elastic properties of the cell and reflects properties of the cell cortex and axoplasm. The other spring, with stiffness k_w, represents the longitudinal effects of a circumferential stiffness of the cell coupled through the incompressibility of the cell contents. If a length H of the cell undergoes a change in circumferential stiffness, k_w, the incompressibility of the cell contents will then ensure that the effect on the length would be equivalent to an additional longitudinal spring of magnitude $k_c = H\,k_w/C$, where $C = 2\pi r$ is the cell circumference. Thus circumferential constriction of the cell would generate an extending force along the cell axis. The internal viscous forces, generated by the cell cortex and the cytoplasmic contents, are represented by γ_{int} and external viscous forces are represented by a damping term γ_{ext}. This model is clearly an over-simplification: no account of the fluid inertia has been taken and, for example, as a lumped model, it

takes no account of the distributed nature of the viscoelastic elements which are likely to account for the observed delay in the movement observed in Fig. 8.

To explain the cell elongation when ruptured, it is supposed that at rest the spring k_l is under compression and that the spring k_w is under tension, so that when ruptured the cell elongates to the natural length of the spring k_l. If k_c is membrane potential dependent, the length will then vary between a fully extended length (L_+) and a fully shortened length (L_-) where the stiffness k_w is maximal (thereby maximally compressing the spring k_l). In this model, therefore, the length is midway between the two extremes when the stiffnesses balance, i.e. $k_c = k_l$. Under these assumptions the steady-state length of the cell will be given by:

$$L = (k_c L_+ + k_l L_-)/(k_c + k_l). \quad (3)$$

where $L_+(L_-)$ is the extended (shortened) length of the cell. If k_c is exponentially dependent on voltage $k_c = A \exp(aV)$ where A and a are constants, and k_l is parametrized as a constant function $k_l = A \exp(aV_0)$, then eqn. (1) can be rewritten as

$$L = L_0 + \Delta L_0 \tanh(a(V - V_0)/2), \quad (4)$$

where $L_0 = (L_+ + L_-)/2$ and is the mid-position of the length change and $\Delta L_0 = (L_+ - L_-)/2$ and is the amplitude of the excursion from L_0. By choosing $a = 19{\cdot}8 \times 10^{-3}\ \mathrm{mV}^{-1} = 1/51\ \mathrm{mV}^{-1}$, determined from the potential sensitivity of the movement (p. 333), and $V_0 = -50$ mV, eqn. (4) fits the experimental data of Fig. 7 over the range which includes the saturation of the movement. Such voltage sensitivity of k_c might suggest that the force-generating mechanism may involve the movement of particles involving one elementary charge in the membrane potential field.

A viscous force, $\gamma_{ext}\, dL/dt$, acting on an isolated cell freely suspended in medium, arises from redistributing fluid around the cell. This force would be in the order of $6\pi r\eta\, dL/dt$ (Stokes relation), where η is the viscosity of the medium with a value of about 1 cP, and r is an effective radius of the cell, which may be taken to be 6 μm. From Fig. 6, the maximum elongation velocity, dL/dt, is 2 μm/ms. The maximum external viscous force in these experiments must therefore have been about 0·22 nN. These considerations suggest that the longitudinal stiffness of a hair cell must exceed 0·1 nN per micrometre extension. This number can be experimentally investigated using methods employed to measure the bundle stiffness (Strelioff & Flock, 1984; Howard & Ashmore, 1986).

The stimulus for outer hair cell motility

The results indicate that outer hair cell length changes must depend either non-selectively on current (but independently of internal calcium) or on a component of the current which is not blocked in these experiments, or upon membrane potential. In cells which showed asymmetric and time-dependent whole-cell currents (e.g. the cell in Fig. 6) there was no detectable asymmetry in the photosensor output. In such experiments, voltage sensitivity was also slightly less variable than current sensitivity, and cells with input conductances between 10 and 40 nS all produced

maximal movements of 4–5% of their length. Finally the length change remains symmetrical about −50 mV (Fig. 7), even when the ionic species within the cell is changed. These considerations suggest that membrane potential may be the controlling factor. Current as the driving force has been suggested previously (Ashmore & Meech, 1986; Ashmore, 1986) but based on smaller excursions of membrane potential, and in experiments in which the pipette access resistance may have varied.

If shape changes are driven by membrane potential, the low-pass cell membrane filter will attenuate these potentials. The inferred time constant for the apical outer hair cells is about 1·5 ms (Fig. 12). In cells from the basal turn, measured *in vivo*, the time constant is about 0/13 ms (Russell, Cody & Richardson, 1986). This filter (overridden in the experiments by the voltage clamp) would reduce the amplitude of forces in apical turn outer hair cells by 19 dB at 1 kHz, and in basal turn cells by about 24 dB at their characteristic frequency. For such reasons it has been suggested that the outer hair cells might be current driven (Russell *et al.* 1986). However, because of the short cable properties of the cell (Jack, Noble & Tsien, 1975; pp. 77–81) the cell is unlikely to be at isopotential when the apical transducer channel is gated at sound frequencies above 1 kHz. In particular membrane potential attenuation would be less at the cell apex. Thus the force-generating mechanism would, in effect, be current sensitive, and at high frequencies not directly limited by the cell time constant.

Mechanism of hair cell movements

The mechanism of rapid changes in outer hair cells is unlikely to arise from hydrostatic forces generated by water movement across the cell membrane. If it is assumed that a 4% increase in length is due solely to an increase in the cell volume (i.e. 0·36 pl for a cell 80 μm in length) then each elementary charge entering the cell during the initial 5 ms would have to be associated with a transfer of about 400 water molecules which seems unrealistically large. Further, since the volume change would be the integral of the charge transfer, the cell volume should have continued to grow. It is possible that subsequent slow (> 40 ms) movements may be associated with electro-osmotic transfer of water, as suggested in the squid axon (Terakawa, 1985). Water transfer thus appears not to be involved over the first 5 ms and other mechanisms must be sought for the rapid component described here.

Because the movements continued in the absence of intracellular ATP and of calcium, a motile mechanism based on actomyosin can be ruled out. On kinetic grounds, movements of outer hair cells are probably too fast to be described by an interaction between actin and myosin, even though such proteins are present in the cell (Flock, 1983). Studies with rapid activation of the cross-bridge cycle by caged ATP (Goldman, Hibberd, McCray & Trentham, 1982) suggest that such interactions are activated over a time course of about 1 ms, and this would have been apparent in the latency measurements. The maximum velocity of shortening of twitch muscle fibres, typically 50 μm/s per sarcomere for the inferior rectus muscle (Luff, 1981), is of about the same magnitude as found here, but unidirectional. Insect muscle can resonate at 3 kHz (Pringle, 1978), but this mechanism has not been described as being driven uniformly over the range of frequencies 0–5 kHz exhibited by outer hair cells. In addition Fig. 8 shows that there is no overshoot of the outer hair cell motion when activated, which would be characteristic of a resonant system.

Other mechanisms of cell motility are known. The vorticellid protozoon *Zoothamnium geniculatum* possesses a contractile arm or 'spasmoneme' which withdraws at a peak rate of about 200 mm/s (172 lengths/s) during about 1 ms (Amos, Routledge, Weis-Fogh & Yew, 1976). This process is calcium dependent, however, and has a slow recovery period. It must thus be based on a different mechanism from outer hair cells where the movement continues to occur even in the presence of 50 mM-internal BAPTA (Ashmore & Meech, 1986). Another non-muscle motile mechanism is found in the acrosomal process of sea urchin sperm which elongates by about 60 μm in 5 s (Tilney & Inoue, 1982). This process is diffusion limited and although actin is present in outer hair cells, it is difficult to see how such a mechanism, actin polymerization, could also be driven into reverse and produce sinusoidal length changes.

Motility in outer hair cells exhibits some similarities in common with rapid pressure changes in squid axons (Tasaki & Iwasa, 1982; Terakawa, 1985) where intracellular pressure rises during an action potential. In these axons, the internal pressure increase is propagated along the axon. The reported changes in diameter and pressure in the axon occur on a submillisecond time-scale, although the ability to follow high frequencies has not yet been reported. The internal pressure changes are measured to be about 30 mPa. To expand against a viscous force of about 0·1 nN, the internal pressure in a hair cell would have to be about 1·4 Pa, or at least 10 times greater than estimated in the squid. Nevertheless, the squid axon pressure changes do occur, as found in hair cells, even when the internal contents of the cell are dialysed.

The most likely mechanism appears to depend on a charge-dependent, or electrostrictive, movement of the cell cortex. Since movement can still be induced when the cell is patched at any site along its length, it must be inferred that it is transmembrane, rather than axial, potential or current which drives the movement. Since the maximum sensitivity of the movement occurs near -50 mV, it is tempting to suggest that the movement may depend on positive charges placed on the inside of the cell cortex, possibly associated with the subsurface cisternae or the 30 nm spaced columnar structures associated with the plasma membrane (Saito, 1983; Flock *et al.* 1986). If these structures are associated with a positive charge, they would be neutralized by inside cell negativity, and give rise, by responding to the electric field, to movements of the cell cortex.

Movements dependent on physiological activity have been reported in turtle hair cells, where lateral deflections of the hair cell bundle have been recorded using microprobe methods (Crawford & Fettiplace, 1985) and in saccular hair cells following stimulation of the efferent fibres (Ashmore, 1984). If both of these types of cell exhibit small voltage- (or current-) dependent movements, lateral movement of the hair bundle tip could occur if the bundle axis did not coincide with the axis of the cell. Such movement would be generated by current flowing through the mechano-electric transducer channel and the observed motion would appear to null at the reversal potential for the transducer channel. Whether the movement reinforced or opposed bundle displacement would then be a property of the geometry of each hair cell.

I thank Professor A. Flock for introducing me to isolated outer hair cells, Drs W. E. Brownell, R. W. Meech and M. C. Holley for helpful discussions, Dr D. Woolley for loan of equipment, and H. Dunn for technical assistance. This work was supported by the Medical Research Council.

REFERENCES

ALLEN, J. B. (1980). Cochlear micromechanics – a physical model of transduction. *Journal of the Acoustical Society of America* **68**, 1660–1670.

AMOS, W. B., ROUTLEDGE, L. M., WEIS-FOGH, T. & YEW, F. F. (1976). The spasmoneme and calcium-dependent contraction in connection with specific binding proteins. In *Calcium in Biological Systems. Symposia of the Society for Experimental Biology XXX*, ed. DUNCAN, C. J., pp. 273–301. Cambridge: Cambridge University Press.

ASHMORE, J. F. (1984). The stiffness of the sensory hair bundle of frog saccular hair cells. *Journal of Physiology* **350**, 20*P*.

ASHMORE, J. F. (1985). Measurement of hair cell movement using a linear position detector. *Journal of Physiology* **364**, 4*P*.

ASHMORE, J. F. (1986). The cellular physiology of the isolated outer hair cells: implications for cochlear frequency selectivity. In *Auditory Frequency Selectivity*, ed. MOORE, B. C. J. & PATTERSON, R. D., pp. 103–108. New York: Plenum Press.

ASHMORE, J. F. & BROWNELL, W. E. (1986). Kilohertz movements in hair cells isolated from the cochlea of the guinea-pig. *Journal of Physiology* **377**, 41*P*.

ASHMORE, J. F. & MEECH, R. W. (1986). Ionic basis of the resting potential in outer hair cells isolated from the guinea pig cochlea. *Nature* **322**, 368–371.

BROWN, M. C. & NUTTALL, A. L. (1984). Efferent control of cochlear inner hair cell responses in the guinea-pig. *Journal of Physiology* **254**, 625–646.

BROWN, M. C., SMITH, D. I. & NUTTALL, A. L. (1983). The temperature dependency of neural and hair cell responses evoked by high frequencies. *Journal of the Acoustical Society of America* **73**, 1662–1670.

BROWNELL, W. E., BADER, C. R., BERTRAND, D. & DE RIBAUPIERRE, Y. (1985). Evoked mechanical responses of isolated cochlear hair cells. *Science* **227**, 194–196.

CODY, A. R. & RUSSELL, I. J. (1985). Outer hair cells in the mammalian cochlea and noise induced hearing loss. *Nature* **315**, 662–665.

CRAWFORD, A. C. & FETTIPLACE, R. (1985). The mechanical properties of ciliary bundles of turtle hair cells. *Journal of Physiology* **364**, 359–380.

DALLOS, P. (1985). Response characteristics of mammalian cochlear hair cells. *Journal of Neuroscience* **5**, 1591–1608.

DALLOS, P., SANTOS-SACCHI, J. & FLOCK, A. (1982). Intracellular recordings from cochlear outer hair cells. *Science* **218**, 582–584.

DAVIS, H. (1965). A model for transducer action in the cochlea. *Cold Spring Harbour Symposia on Quantitative Biology* **30**, 181–190.

DAVIS, H. (1983). An active process in cochlear mechanics. *Hearing Research* **9**, 79–90.

DE BOER, E. (1983). No sharpening? A challenge for cochlear mechanics. *Journal of the Acoustical Society of America* **73**, 567–573.

EVANS, E. F. & HARRISON, R. V. (1976). Correlation between outer hair cell damage and deterioration of cochlear nerve tuning properties in the guinea pig. *Journal of Physiology* **256**, 43–44*P*.

FLOCK, A. (1983). Hair cells, receptors with a motor capacity? In *Hearing – Physiological Bases and Psychophysics*, ed. KLINKE, R. & HARTMANN, R., pp. 3–7. Berlin: Springer-Verlag.

FLOCK, A., FLOCK, B. & ULFENDAHL, M. (1986). Mechanisms of movement in outer hair cells and a possible structural basis. *Archives of Otorhinolaryngology* **243**, 83–90.

GEISLER, C. D. (1986). A model of the effect of outer hair cell motility on cochlear vibrations. *Hearing Research* **24**, 125–132.

GOLDMAN, Y. E., HIBBERD, M. G., MCCRAY, J. A. & TRENTHAM, D. R. (1982). Relaxation of muscle fibres by photolysis of caged ATP. *Nature* **300**, 701–705.

GUMMER, A. W. & JOHNSTONE, B. M. (1981). Direct measurements of the basilar membrane stiffness in the guinea pig. *Journal of the Acoustical Society of America* **70**, 1298–1309.

HAMMILL, O., MARTY, A., NEHER, E., SAKMANN, B. & SIGWORTH, F. J. (1981). Improved patch-clamp techniques for high resolution current recording from cells and cell-free membrane patches. *Pflügers Archiv* **391**, 85–100.

HOWARD, J. & ASHMORE, J. F. (1986). The stiffness of hair bundles of the frog sacculus. *Hearing Research* **23**, 93–104.

JACK, J. J. B., NOBLE, D. & TSIEN, R. W. (1975). *Electric Current Flow in Excitable Cells*. Oxford: Oxford University Press.

KHANNA, S. M. & LEONARD, D. (1982). Basilar membrane tuning in the cat cochlea. *Science* **215**, 305–306.

LAMB, T. D., MATTHEWS, H. R. & TORRE, V. (1986). Incorporation of calcium buffers into salamander retinal rods: a rejection of the calcium hypothesis of phototransduction. *Journal of Physiology* **372**, 315–350.

LIBERMAN, M. C. & DODDS, L. W. (1984). Single neuron labelling and chronic cochlear pathology. II. Stereocilia damage and alterations in the spontaneous discharge rates. *Hearing Research* **16**, 43–53.

LIM, D. J. (1980). Cochlear anatomy related to cochlear micromechanics. A review. *Journal of the Acoustical Society of America* **67**, 1686–1695.

LIM, D. J. & FLOCK, A. (1985). Ultrastructural morphology of enzyme-dissociated cochlear sensory cells. *Acta otolaryngologica* **99**, 478–492.

LUFF, A. R. (1981). Dynamic properties of the inferior rectus, extensor digitorum longus, diaphragm and soleus muscles of the rat. *Journal of Physiology* **313**, 161–172.

NEELY, S. T. (1983). The cochlear amplifier. In *Mechanics of Hearing*, ed. DE BOER, E. & VIERGEVER, M. A., pp. 111–118. Delft: Martinus Nijhoff.

NEELY, S. T. & KIM, D. O. (1986). A model for active elements in cochlear biomechanics. *Journal of the Acoustical Society of America* **79**, 1472–1480.

MAGLEBY, K. L. & PALOTTA, B. S. (1983). Calcium dependence of open and shut interval distributions from calcium-activated potassium channels in cultured rat muscle. *Journal of Physiology* **344**, 585–604.

MILLER, C. E. (1985). Structural implications of basilar membrane compliance measurements. *Journal of the Acoustical Society of America* **77**, 1465–1474.

PRINGLE, J. S. (1978). Stretch activation of muscle: function and mechanism. *Proceedings of the Royal Society* B **201**, 107–130.

RHODE, W. S. & GEISLER, D. (1967). Model of the displacement between opposing points on the tectorial membrane and reticular lamina. *Journal of the Acoustical Society of America* **42**, 185–190.

RUSSELL, I. J., CODY, A. R. & RICHARDSON, G. P. (1986). The responses of inner and outer hair cells in the basal turn of the guinea pig cochlea and in the mouse cochlea grown *in vitro*. In *Cellular Mechanisms of Hearing, Nobel Symposium* 63, ed. FLOCK, A. & WERSALL, J., pp. 199–216. Amsterdam: Elsevier.

RUSSELL, I. J. & SELLICK, P. M. (1983). Low-frequency characteristics of intracellularly recorded receptor potentials in mammalian hair cells. *Journal of Physiology* **338**, 179–206.

SAITO, K. (1983). Fine structure of the sensory epithelium of guinea-pig organ of Corti: subsurface cysterna and lamellar bodies in the outer hair cells. *Cell and Tissue Research* **229**, 467–481.

SELLICK, P. M., PATUZZI, R. & JOHNSTONE, B. M. (1982). Measurement of basilar membrane motion in the guinea pig using the Mossbauer technique. *Journal of the Acoustical Society of America* **72**, 131–141.

STRELIOFF, D. & FLOCK, A. (1984). Stiffness of sensory-cell hair bundles in the isolated guinea-pig cochlea. *Hearing Research* **15**, 19–28.

TASAKI, I. & IWASA, K. (1982). Rapid pressure changes and surface displacements in the squid giant axon associated with the production of action potentials. *Japanese Journal of Physiology* **32**, 69–81.

TERAKAWA, S. (1985). Potential-dependent variations of the intracellular pressure in the intracellularly perfused squid giant axon. *Journal of Physiology* **369**, 229–248.

TILNEY, L. G. & INOUE, S. (1982). Acrosomal reaction of thyone sperm. II. The kinetics and possible mechanism of acrosomal process elongation. *Journal of Cellular Biology* **93**, 820–827.

ZENNER, H. P., ZIMMERMAN, U. & SCHMIDT, U. (1985). Reversible control of isolated mamalian cochlear hair cells. *Hearing Research* **18**, 127–134.

ZWISLOCKI, J. J. (1980). Five decades of research on cochlear micromechanics. *Journal of the Acoustical Society of America* **67**, 1679–1685.